# Direct Spectroscopic Observation of the Energy Gap Formation in the Spin Density Wave Phase Transition at the Cr(110) Surface

J. Schäfer,[1,2] Eli Rotenberg,[1] G. Meigs,[1] and S. D. Kevan[2]
[1]*Advanced Light Source, Lawrence Berkeley National Laboratory, Berkeley, California 94720*
[2]*Department of Physics, University of Oregon, Eugene, Oregon 97403*

P. Blaha
*Institut für Physikalische und Theoretische Chemie, Technische Universität Wien, 1060 Wien, Austria*

S. Hüfner
*Fachbereich Physik, Universität des Saarlandes, 66041 Saarbrücken, Germany*
(Received 28 May 1999)

The spin density wave phase transition in chromium has been studied by angle-resolved photoemission on a (110) surface. The electronic band structure is shown to exhibit backfolding in the antiferromagnetic state. Direct spectroscopic evidence is obtained on the gradual opening of an energy gap at the Fermi level. The gap extends almost isotropically around the $\Gamma$ point, its magnitude reaching $\sim$200 meV at room temperature. Density-functional band structure calculations confirm the location of the energy gap in reciprocal space and yield enhanced magnetic moments towards the surface. The transition probed in the near-surface layers exhibits a critical temperature of $\sim$440 K.

PACS numbers: 75.30.Pd, 71.15.Mb, 71.18.+y, 75.30.Fv

The formation of a spin density wave (SDW) ground state in some metals continues to challenge our fundamental understanding of magnetic interactions. For example, the well-known incommensurate SDW state in Cr [1] is thought to play a major role in the interlayer coupling observed in Fe:Cr multilayers, where both short- and long-range periodicities are observed in the giant magnetoresistance effect [2]. However, Cr is in fact only marginally magnetic, since the Fermi level ($E_F$) lies near a minimum in the density of states. The generalized Stoner criterion for the product of electron interaction energy and generalized susceptibility, $U \cdot \chi(\mathbf{q}_{\mathrm{SDW}}) > 1$, is barely satisfied [3]. Any change in the band structure near $E_F$ accompanying the paramagnetic (PM) to antiferromagnetic (AFM) transition must on these grounds be very small. The formation of an SDW leads to an energy gap $\Delta$, which in weak-coupling mean-field theory [4] at $T = 0$ is $\Delta = 3.53kT_N$, where $T_N$ is the Néel temperature.

What is the actual magnitude and extent of the energy gap of the SDW that has such a pronounced impact on material properties? Experimental indication that the formation of the SDW leads to considerable reduction in the size of the Fermi surface came originally from anomalous skin effect [5] and de Haas–van Alphen [6] measurements. Data on the bulk energy gap, which has importance as an order parameter, come from infrared measurements of Machida *et al.* [7], which determine a low temperature band gap of $\sim$120 meV. With the established bulk transition temperature of 311 K [1], this indicates that mean-field theory with a predicted gap of 95 meV is a reasonable approximation. However, the crucial points of where exactly in $k$ space the gap forms, what magnitude it assumes in the vicinity of a surface, and its behavior with temperature are largely unclear to date. Attempts at a determination of the band structure from photoemission were undertaken [8–10], but the problems of surface contaminants and insufficient resolution were encountered. This rendered them so far inconclusive, and an energy gap or a transition temperature could not be established.

In this Letter, we present angle-resolved photoelectron spectroscopy (ARPES) data with high momentum and energy resolution on clean Cr(110) thin films that provide electronic band structure data, and supplement these measurements with surface band structure calculations. For the first time, direct evidence of the band structure backfolding, magnitude, and extent of the energy gap is presented. The behavior of the order parameter is also studied as a function of temperature.

The ARPES experiments were carried out at beam line 7.0 at the Advanced Light Source. The energy resolution used was $\sim$50 meV; the momentum resolution was $\sim 0.03 \times 2\pi/a$, with $a = 2.88$ Å the lattice constant of Cr. The Cr(110) surface was prepared in ultrahigh vacuum by evaporation of $\sim$100 layers of Cr onto a clean W(110) crystal and subsequent annealing. From a measurement of the size of the Brillouin zone (BZ), the Cr film surface was found to be strain-free. The crystal perfection was judged from a $(1 \times 1)$ LEED pattern as well as from the sharp photoemission features.

Previous work [1,6] has predicted that the Fermi surface nesting wave vector relevant to SDW formation, $\mathbf{q}_{\mathrm{SDW}}$, occurs between the electron "octahedron" at $\Gamma$ and the hole "octahedra" at the six H points. The structures are of very similar shape and curvature, as drawn schematically in Fig. 1. By scanning the photon energy, we verified

  

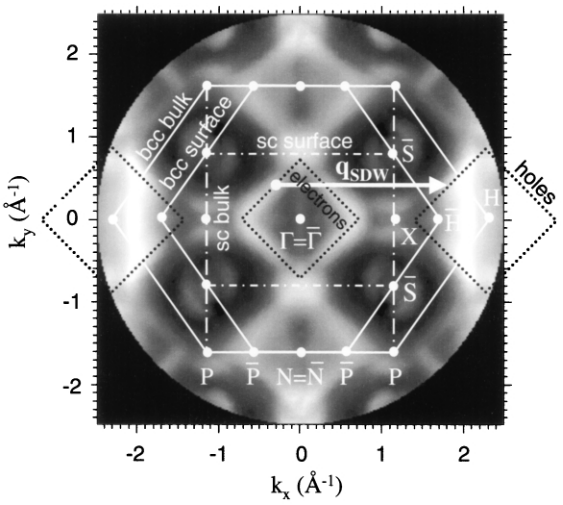


FIG. 1. Surface BZ and bulk BZ intersected at $\Gamma$, superimposed on ARPES Fermi level intensity plot (400 meV window centered at $E_F$, image symmetrized from a 90° sector, $T = 180$ K). SDW nesting occurs between the electron jack at $\Gamma$ and the hole jack at H. The data provide an estimate for $\mathbf{q}_{\mathrm{SDW}} = 0.95 \pm 0.05\Gamma$-H.

from the band structure symmetry that at $h\nu = 119.6$ eV the bulk BZ is intersected approximately at $\Gamma$ ($k_\perp \sim 6$ Å$^{-1}$). By measuring the photoemission intensity at $E_F$ as a function of polar and azimuthal angles, we produced the experimental Fermi level data in Fig. 1. From these data we identify the nesting vector $\mathbf{q}_{\mathrm{SDW}} \sim 0.95\Gamma$-H, which is in good agreement with neutron scattering measurements [11].

Band structure calculations provide a useful guide concerning where to look for the SDW gap. While in reality the SDW spans ~27 lattice constants [11], the alternating magnetization of neighboring atoms can be described approximately in a doubled unit cell. We consider a body-centered-cubic (bcc) BZ for the PM phase and a half-size simple cubic (sc) BZ for the AFM phase which effectively leads to backfolding of the electronic band structure. While calculations for Cr have been performed earlier [12,13], the need in the present work is to identify the SDW gap in those near-surface layers that we probe by photoemission (exponential attenuation with mean escape depth of ~5 Å), and in an experimentally suitable direction. The exchange interaction is sensitive to the electronic valence configuration, and thus the Cr surface magnetic properties and the transition temperature can be expected to differ markedly from the bulk.

We have calculated the band structure of PM and AFM Cr both for the bulk and a nine-layer slab at the surface, using the density-functional theory within the generalized gradient approximation (GGA) [14] and a relativistic self-consistent full-potential linearized augmented plane wave procedure [15]. In addition, bulk properties were also derived in the local spin density approximation (LSDA). From the symmetry of the BZ's in Fig. 1 it is apparent that the $\bar{\Gamma}$-$\bar{S}$ direction stands out, in that it is normal to the nested Fermi surface section, hence expected to give a very clearcut view. The GGA calculations for this direction are shown in Fig. 2(a). The bulk gap formation occurs at a distance of ~40% away from $\Gamma$ towards $\bar{S}$. The slab calculation on the right side of Fig. 2(a) exhibits many bands that are surface-modified bulk states and a few bands that are genuine surface states located in a large projected band gap. The gap obtained for the antiferromagnetic surface state bands is located at the same momentum as the bulk gap and of magnitude $\Delta \sim 0.3$ eV, as compared to ~1.0 eV for the subsurface layers and the bulk (0.5 eV in LSDA). From the surface slab calculation we obtain magnetic moments for the topmost three layers that are enhanced by factors of 1.72, 1.14, and 1.05 relative to the bulk moment of $1.15\mu_B$. The latter is significantly larger than both the experimental [1] and the theoretical value calculated within LSDA of $0.62\mu_B$. The strong dependence of the magnetic moment in Cr on the particular exchange-correlation potential was already pointed out by Singh and Ashkenazi [16].

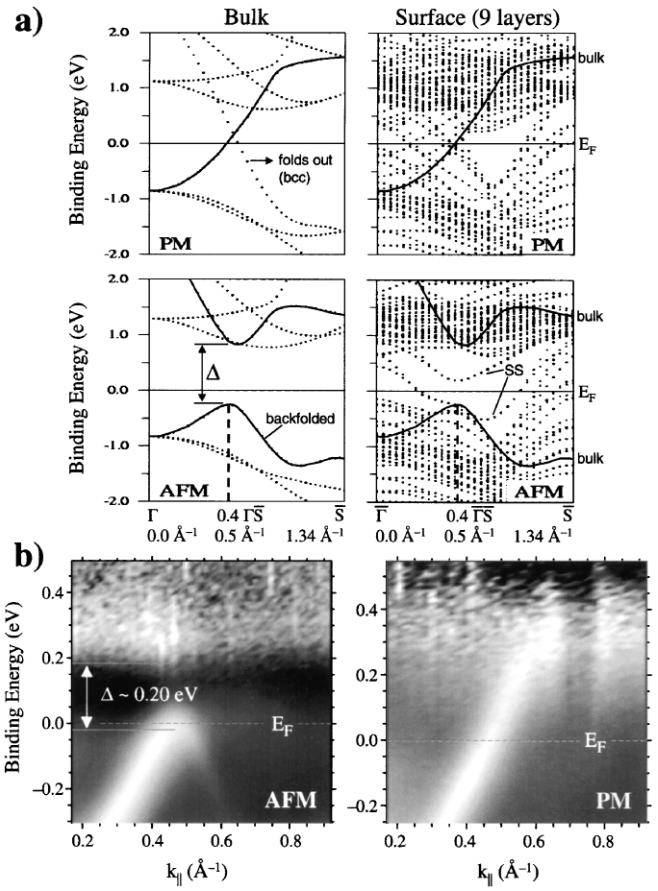


FIG. 2. (a) GGA band structure calculation for bulk (left) and nine-layer surface slab (right), including surface states (SS). The PM band structure is drawn backfolded into the sc BZ. The SDW energy gap $\Delta$ is consistently predicted at $0.4\bar{\Gamma}$-$\bar{S}$. (b) Band maps along $\bar{\Gamma}$-$\bar{S}$ taken at 300 K (left) and 570 K (right), with the Fermi distribution divided out.

Experimental band maps with fixed $k_\perp$ (6 Å$^{-1}$) and with $k_\parallel$ varied along $\overline{\Gamma}$-$\overline{S}$ were taken at temperatures far below ($T = 300$ K) and above ($T = 570$ K) the measured surface Néel temperature (440 K; see below). The raw data after subtraction of a smooth background were divided by the Fermi distribution $f(E)$ to allow observation of thermally excited states above the Fermi level [Fig. 2(b)]. To accommodate the experimental resolution and phonon broadening, we augmented the temperature in $f(E)$ with a small constant energy term, thus modeling the Fermi edge intensity drop of our apparatus. The dangling-bond surface state is too weak to be seen in Fig. 2(b) compared to the more bulklike states of the deeper layers, especially considering how quickly the surface state intensity deteriorates even under ultrahigh vacuum conditions. We observe at low temperature (i) a second branch emerges that is rising from $\overline{S}$ and (ii) a diffuse intensity above $E_F$, which we identify with the band above the SDW gap. This identification is completely confirmed from measurements throughout the surface BZ (see Fig. 3 and discussion below). The band structure is thus exhibiting an almost direct gap at $E_F$ which we determine to be 200 ± 20 meV. The additional branch is identified with the aid of the calculation as resulting from the BZ reduction ("backfolded" branch). The gap formation occurs at a distance of ~0.40 away from $\overline{\Gamma}$ towards $\overline{S}$ as predicted by the calculation, while the model overestimates the energy gap $\Delta$. The observed magnitude of the energy gap is larger than the bulk value of 120 meV reported from infrared measurements [7].

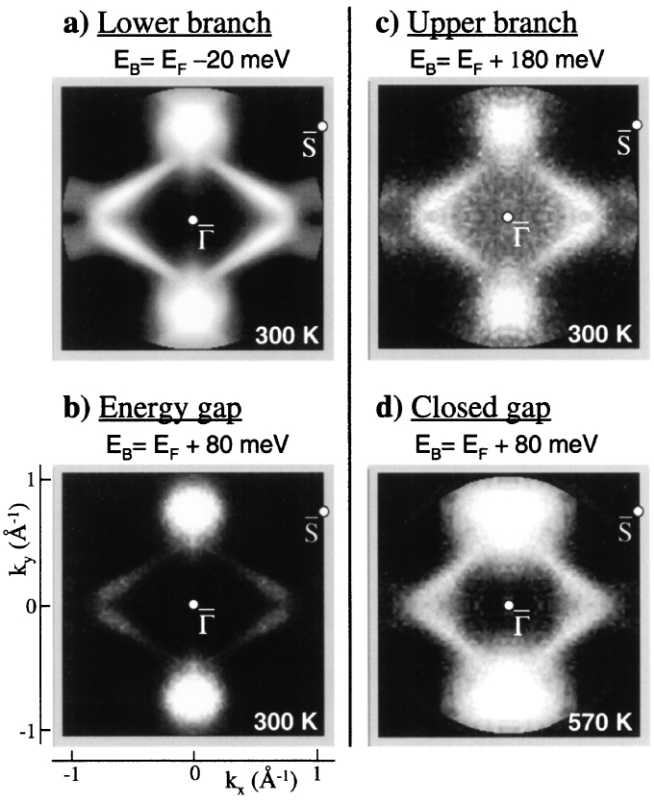


FIG. 3. Constant binding energy ARPES without energy integration other than the experimental resolution [intensity calibrated with Fig. 2(b)]. In the SDW-nested AFM state, (a) and (c) represent the edges of the bands that define the virtually isotropic SDW gap seen in (b) of ~200 meV, which is filled in the PM state (d).

In Fig. 3 we present constant energy contours obtained from ARPES in the vicinity of $E_F$ in the AFM and PM states. The data represent $k$-space maps of states at energies corresponding to (a) the lower edge, (b) the middle, and (c) the upper edge of the gap in the SDW phase ($T = 300$ K), as well as (d) the middle of the gap region in the PM phase ($T = 570$ K). These data show graphically that the energy gap opens almost isotropically and with constant magnitude of 200 ± 20 meV around this section of the electron octahedron at $\Gamma$. This finding of an isotropic energy gap is consistent with our band structure calculations.

We also monitored the order parameter of the phase transition by measuring the temperature dependence of the energy gap. The result of this series, again after elimination of the Fermi distribution, is shown in Fig. 4(a). The edge of the lower band clearly tracks the gradual closure of the gap. From examination of the numerous individual band maps, a surface transition temperature of $T_N^S = 440 \pm 10$ K is determined, considerably above the bulk Néel temperature of $T_N^{\mathrm{Bulk}} = 311$ K. The temperature dependence of the lower section of the SDW energy gap is plotted in Fig. 4(b). The data can be represented quite well over a relatively wide temperature range by a power law $(1 - T/T_N)^\beta$ with $\beta = 0.38 \pm 0.05$. The exponent was obtained using a window of 140 K below the transition, yet remains also within the specified error bar if a much smaller region is fitted.

Towards the surface, on the basis of the calculated increase of the magnetic moments, SDW mean-field theory lets us qualitatively expect a larger energy gap and a higher transition temperature, as is observed. Although short-range magnetic order might persist above $T_N^{\mathrm{Bulk}}$ [17], from bulk studies this is not known to lead to an energy gap [1,7]. The existence of a gap near the surface up to a sharply defined $T_N^S$ rather has the signature of a phase transition. For the critical behavior, the SDW weak-coupling limit which is based on the Heisenberg Hamiltonian yields a critical exponent of 0.5 in a three-dimensional (3D) system. Motivation for looking into 2D systems comes from the confined near-surface enhancement of the magnetic moment and the possibility of a distinct surface transition. However, at finite temperatures magnetic order in one or two dimensions is prohibited in the simple Heisenberg model by quantum fluctuations. Experiments on the critical behavior of a ferromagnetic thin film, using Ni(111) on W(110), show a crossover from 3D behavior to 2D behavior between seven and four monolayers [18]. This crossover leads to a reduction of the critical exponent, an

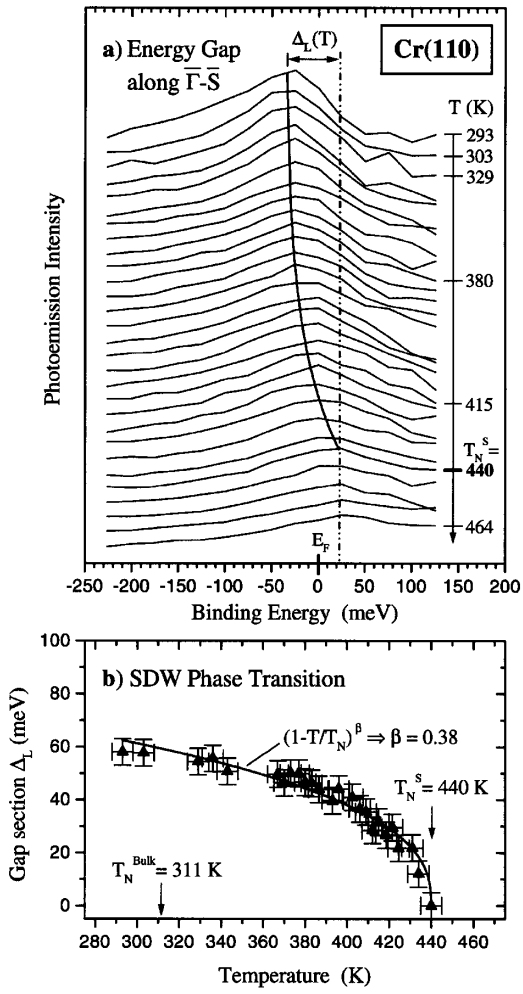


FIG. 4. (a) Temperature series of SDW energy gap spectra, extracted from wider $k$-window band maps (Fermi distribution divided out). The gap closes at 440 K judged from the individual band maps. (b) Lower section of the SDW energy gap obtained from a Lorentzian fit to the spectra in (a). The critical behavior near the surface phase transition can be fitted with a power law.

observation that likely might hold for the present system as well.

Concerning the order of the transition, the SDW description mentioned above predicts a continuous, second order transition. However, in looking at the critical behavior of the bulk magnetization from neutron scattering [1], it is inferred that the transition in bulk Cr is of weak first order, with a very small discontinuity at $T_N^{\mathrm{Bulk}}$. The data shown in Fig. 4(b) are compatible with such a small discontinuity to the first or second data point below the transition. The SDW transition can be modeled as of first order if electron-phonon coupling is introduced [19]. At the surface, however, the crucial relative strength of the electron-phonon coupling with respect to the enhanced magnetic moments may be different from the bulk.

In summary, with this study of the SDW phase transition at the Cr(110) surface we have derived spectroscopic information about the SDW energy gap. The gap of ~200 meV magnitude covers essentially the entire measured section of the electron octahedron. An increased (110) near-surface transition temperature of 440 K is found, with the approach of the order parameter essentially continuous and power-law-like. While this work grants insight into the formation of the energy gap near the surface, we suggest that future research could help elucidate the question of magnetic moments and electron-phonon coupling at the surface.

The authors are grateful to J. D. Denlinger for valuable scientific discussion. This work was supported by the U.S. DOE under Grant No. DE-FG06-86ER45275 and by the ALS under Grant No. DE-AC03-76SF00098.

[1] E. Fawcett, Rev. Mod. Phys. **60**, 209 (1988), and references therein.
[2] D. Li *et al.*, Phys. Rev. Lett. **78**, 1154 (1997).
[3] H. L. Skriver, J. Phys. F **11**, 97 (1981).
[4] P. Fazekas, *Lecture Notes on Electron Correlation and Magnetism* (World Scientific, Singapore, 1999).
[5] E. Fawcett and D. Griffiths, J. Phys. Chem. Solids **23**, 1631 (1962).
[6] J. Graebner and J. A. Marcus, J. Appl. Phys. **37**, 1262 (1966).
[7] K. Machida, M. A. Lind, and J. L. Stanford, J. Phys. Soc. Jpn. **53**, 4020 (1984).
[8] P. E. S. Persson and L. I. Johansson, Phys. Rev. B **34**, 2284 (1986).
[9] L. E. Klebanoff *et al.*, J. Magn. Magn. Mater. **54–57**, 728 (1986).
[10] Y. Sakisaka *et al.*, Phys. Rev. B **38**, 1131 (1988).
[11] S. A. Werner, A. Arrott, and H. Kendrick, Phys. Rev. **155**, 528 (1967).
[12] S. Asano and J. Yamashita, J. Phys. Soc. Jpn. **23**, 714 (1967).
[13] R. H. Victora and L. M. Falicov, Phys. Rev. B **31**, 7335 (1985).
[14] J. P. Perdew, K. Burke, and M. Ernzerhof, Phys. Rev. Lett. **77**, 3865 (1996).
[15] P. Blaha, K. Schwarz, and J. Luitz, WIEN97 code [improved version of B. Blaha *et al.*, Comput. Phys. Commun. **59**, 339 (1990)].
[16] D. Singh and J. Ashkenazi, Phys. Rev. B **46**, 11 570 (1992).
[17] B. Sinkovic, B. Hermsmeier, and C. S. Fadley, Phys. Rev. Lett. **55**, 1227 (1985).
[18] Y. Li and K. Baberschke, Phys. Rev. Lett. **68**, 1208 (1992).
[19] A. Kotani, J. Phys. Soc. Jpn. **39**, 851 (1975).